International Journal of Mining Science and Technology 31 (2021) 365–375

Contents lists available at ScienceDirect

International Journal of Mining Science and Technology

journal homepage: www.elsevier.com/locate/ijmst

A flexible multi-body model of a surface miner for analyzing the interaction between rock-cutting forces and chassis vibrations

Alessandro Medolago [a], Stefano Melzi [b,*]

[a] Tesmec S.p.A., Grassobbio 24050, Italy
[b] Department of Mechanics, Politecnico di Milano, Milano 20156, Italy

ARTICLE INFO

Article history:
Received 2 September 2020
Received in revised form 7 February 2021
Accepted 15 March 2021
Available online 27 March 2021

Keywords:
Surface miner
Flexible multi-body model
Validation
Cutting forces
Chassis vibrations

ABSTRACT

The discontinuous nature of rock cutting can easily cause unwanted vibrations in the structure of a surface miner. If these vibrations are not properly addressed, the related stress cycles can gradually damage the chassis resulting in fatigue failures. These events can seriously undermine the safety of operators and digging operations may be stopped for days, with an obvious economic impact. This work presents an analysis of the dynamics of a surface miner, focusing on the interaction between cutting machine dynamics and cutting forces, which is a new approach for this type of machine. For this purpose, the authors developed a numerical model of the cutting process made up of (1) a multi-body model of the cutting machine, which takes into account the chassis's flexibility; (2) a model of the rotating cutting head; and (3) a model of the interaction between the cutting head and rock, based on Shao's model. The model was compared with experimental results and then used to investigate the effects of cutting speed and cutting depth on the machine dynamics.

1. Introduction

Excavation, the process of moving rock or other materials, has been employed since the beginning of civilization for several purposes. The principal material removal technique was by mechanical means until the invention of explosives (the first-known use of which dates back to 1627 [1]) and the development of new types of mechanized excavation equipment. Today, mechanical tools and blasting are used in excavation works for several important applications, including exploration, environmental restoration, mining, and construction. What makes mechanic excavation techniques more appealing than "drill and blast", under the right circumstances, are their increased productivity, environmentally friendly operations, ease of automation, continuous and selective mining, controllability of the chip size, and higher safety [2–5]. For instance, the implementation of highwalls is a common practice, in the effort to increase the productivity of surface mines; anyway, highwall stability can be negatively influenced by the use of blasting [6].

Since mechanical excavation efficiency is crucial to several industrial sectors, the scientific community was pushed to develop a new discipline called "rock-cutting mechanics", born in the early 1950 s [7]. Since then, researchers have been focusing on predicting excavation forces, characterizing process efficiency and forecasting equipment productivity [8–10], both in rock and coal excavation [11,12]. To achieve a better comprehension of the mechanics of rock cutting, a large quantity of models has been developed, ranging from theoretical [11–14] to semi-empirical [15,16] and to numerical ones, which simulate the rock fracturing phenomena. Over the past ten years, several types of numerical methods, like the finite element method (FEM) [17], the discrete element method (DEM) [18–20], and hybrid formulations [21] have been used in the analysis of the rock cutting process, and in the mining sector in general [22]. The one that delivers the most promising results, in terms of both accuracy and capability to give a useful insight into the process's mechanics, is DEM. Among the different works in this field, the one by Rojek et al. [19] showed notable results for the simulation of cutting using conical picks. On a larger scale, the study of process-induced vibrations [23] has also been addressed, because of its economic relevance and safety implications.

There are, however, still some open points, especially in terms of predicting the loads acting on the excavation equipment and the tools during the cutting process. In particular, the discontinuous nature of rock cutting can easily cause undesirable vibrations in the machine's structure. Research studies on different excavation machines [24–26] point out the role of multi-point impact

* Corresponding author.
E-mail address: stefano.melzi@polimi.it (S. Melzi).

https://doi.org/10.1016/j.ijmst.2021.03.006
2095-2686/

loads in determining significant vibrations that propagate from the cutterhead to the components of the transmission and the chassis. The authors of literature [24] underline that the position of the boom of a roadheader has a strong influence on vibration levels. A correct position improves the performance of the machine as well as its reliability. The same paper suggests monitoring vibration levels for fault diagnosis. Continuously-variable loads are considered as the cause of cracking of a TBM cutterhead and failure of the main bearing [25]. The work in literature [26] reports experimental data related to accelerations measured on the chassis of a bucket-excavator; vibrations caused the failure of both the platform and the structural base. The authors conclude that correct designing and dimensioning of the structure cannot rely on static analysis alone.

A critical operating condition occurs when periodicities of the cutting forces lead to resonance excitations of eigenmodes in the structure. This phenomenon has been extensively investigated in the field of metal milling [27–30], where the main focus is the effect of vibrations on the surface quality of the cut pieces. In the rock-excavation process on the other hand, the main interest is in the structural integrity of the cutting machine. Resonance excitation is associated with stress cycles that can gradually damage the chassis resulting in fatigue failures. These events can seriously undermine the operators' safety; besides, digging operations may be stopped for days, with significant economic impacts.

This work focuses on the dynamics of the Tesmec 1150XHD RH surface miner (Fig. 1). The goal of the investigation is to develop a better understanding of the interaction between the cutting forces and the dynamics of the cutting machine, with particular reference to the vibration of its chassis, as a function of cutting parameters such as forward speed and cutting depth. In the long-term, the outcome of this research is expected to improve the design process for surface miners, based on a better knowledge of the load cycles associated with different operating conditions. Moreover, given the relevant role that emerging digital technologies are taking on in the mining industry [31], an improved knowledge of the machine dynamics of this type could also improve predictive maintenance and monitoring algorithms.

The core of this research activity is a multi-body model of the surface miner, able to describe its dynamics, including the effects of the chassis's flexibility. The model, developed using the ADAMS commercial software, interacts in co-simulation with a MATLAB/Simulink model, which computes the excavation forces on the basis of the relative motion between the cutting head and the rocky soil. A semi-empirical model is adopted for estimating the cutting forces, making it possible to combine realistic predictions with a low computational load. Though having proved to be a very accurate way of modelling the rock breaking process, large scale DEM simulations are still too expansive in terms of computational load. A semi-empirical model was thus preferred for this kind of application. Altogether, the numerical model allows designers to consider the effects of excavation forces on the dynamic response of the surface miner which, in turn, influences the motion of the cutting head and the magnitudes of these forces.

Using multi-body models to describe the dynamics of operating machines is quite common in the field of soft-soil mechanics. These models are applied to predict tractive performance [32,33], operator comfort [34], interactions between tools and soil [35] and even for developing real-time simulators for training purposes [36]. To the authors' knowledge, the same approach is not so popular when dealing with rock mechanics: as mentioned above, considerable results were obtained in the prediction of cutting forces associated with rock chipping and fragmentation. However, when the interaction between tools and rock is simulated, the motion of the cutting tool is often assumed to be ideal, i.e., the dynamics of the supporting structure is overlooked [21,37].

In this work, however, the dynamics of the surface miner is a key element: numerical simulations are used to show how the periodicity of cutting forces can produce resonance excitation of the chassis. The mutual interaction between machine dynamics and cutting forces can give rise to vibrations of significant amplitude, especially for some operating conditions. The results of the numerical model are validated against experimental data collected in outdoor tests.

This paper is organized as follows: Section 2 describes the main features of the 1150XHD RH cutting machine; Section 3 focuses on the numerical model of the interaction between the machine and the rock, during the cutting process; Section 4 presents a series of comparisons between numerical and experimental data, used to validate the numerical model and understand the benefits of including the effect of chassis dynamics; moreover, the same Section 4 reports a preliminary sensitivity analysis performed using the numerical model.

2. Description of the surface miner

The 1150XHD RH surface miner made by Tesmec (Fig. 1) has a wide range of applications, such as excavation of big channels (e.g. large diameter pipelines), surface mining, bulk excavation and soil reclamation.

The machine is fitted with a rear rotating cutter head (or drum) moved and supported by a track-mounted tractor. The rotating drum is installed at the end of a tilting arm, whose rotation along a transversal axis is controlled by two hydraulic actuators. The rotating motion of the cutter head is obtained via a chain transmission. The chain itself and the drum are fitted with picks designed for the excavation process.

Fig. 2 schematically depicts the cutting drum and the cutting process; parameters like the machine forward speed v_{tract}, the angular speed of the drum ω_{drum} and the radial immersion of the drum d_{drum} are set by the user. The interaction between the picks and the rocky soil determines the formation of grooves and, with reference to Fig. 2, the spacing between the grooves s and the depth of cut doc depends on the relative position between the cutter head and soil, the geometry of the picks and their distribution on the drum surface, as well as on drum operating parameters. Dif-

Fig. 1. Tesmec 1150XHD RH surface miner.

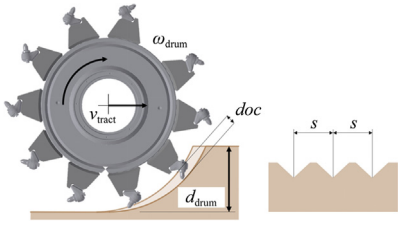

Fig. 2. Legend of the digging process parameters used in this work.

ferent types of picks can be mounted on the cutter head, according to the working conditions.

The machine is powered by a 336-kW diesel engine and has total weight close to 53 t. The diesel engine power is transmitted by a hydraulic transmission and specifically-designed cutting tools carry out the rock breaking.

As mentioned before, this analysis aims to investigate the interaction between cutting forces and vibrations of the chassis. Following the experience developed in the field of metal milling, cutting forces (obtained with a constant angular speed of the drum) may present periodicities that almost overlap the machine's eigenfrequencies. Therefore, resonance excitation may occur, causing the cutting head to move at specific frequencies. Such a response amplifies the same harmonic components of the cutting forces, giving rise to a self-excitation mechanism. It is, therefore, useful to characterize the machine's vibrating response, so that it can be introduced into a mathematical model. The first step consists of determining the chassis's eigenfrequencies and eigenmodes.

A finite-element (FE) model of the chassis was developed in ANSYS; a sketch of the model mesh is shown in Fig. 3. The 1150XHD RH is a large assembly, mainly composed of welded steel parts. During its regular use, the hydraulic cylinders controlling the boom angle remain fixed in the set position and the tractor travelling velocity is very low. All these elements make the system's dynamics largely dependent on the structure's elasticity. Accurate modelling of the system's flexibility is therefore fundamental to the study of its dynamic behaviour, and this can be achieved by a complete FE model of the whole machine. Fig. 3 shows the machine's FE geometry, where all the structural elements are reproduced. The non-structural ones were included in the model by using idealised masses. The joints were modelled to be ideal and the boom's hydraulic cylinders were replaced with springs. In particular, the stiffness of these springs was computed using Eq. (1), i.e., as that of the oil column contained in the cylinder (because, once the actuator is in the digging position, the two chambers' valves are closed).

$$k_{\text{cyl.eq}} = \left(\frac{A_1^2}{V_1} + \frac{A_2^2}{V_2}\right)\varepsilon_e \tag{1}$$

where $k_{\text{cyl.eq}}$ is the hydraulic cylinder equivalent stiffness; A_1, A_2, V_1, V_2 the section areas and the volumes of the two chambers of the cylinder; and ε_e the oil bulk modulus, taken as 1.8×10^9 N/m^2, according to the characteristics of the hydraulic oil used.

The model's mesh was validated using convergence analysis, to guarantee that the structure's flexibility was properly captured. The model is made of a total of nearly 355000 elements, with linear shape functions.

A linear modal analysis was carried out with the FE model to determine the most relevant eigenfrequencies and mode shapes. For both their participating mass and their influence on the structural stresses, these were located in the 3–20 Hz interval. This response is due to a combination of the frame's high-flexibility and the machine's mass-distribution (Fig. 4). The following can be stated:

(1) The lowest mode at 3 Hz is mainly characterized by the movement of the engine assembly's mass.
(2) Two pitch modes are found at about 5 and 10 Hz. The first is characterized by a significant displacement of the boom, while the second features a distributed flexure frame.
(3) The modes at higher frequency appear to be associated with a local deformation of the chassis.

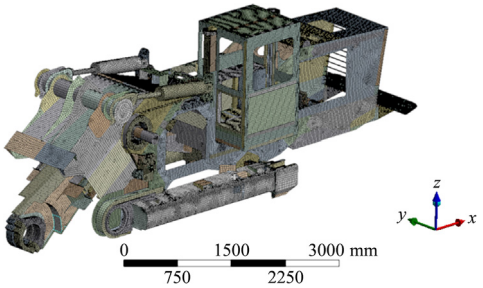

Fig. 3. ANSYS FE model of the surface miner.

3. Numerical modelling

The main target of this work is to develop a better understanding of the interaction between the cutting forces and the machine's dynamics. A numerical model able to reproduce the cutting process, taking into account both these aspects, was then set up. This numerical model consists of two sub-models developed with different simulation environments: an ADAMS multi-body model to describe the dynamics of the surface miner, and a MATLAB/Simulink model to compute the cutting forces. The two sub-models are co-simulated and interact as shown in the diagram in Fig. 5.

The ADAMS model computes the dynamics of the machine, taking into account the flexibility of the chassis, on the basis of the forces exchanged with the rocky soil. These forces are associated with the contact between the tracks and the ground and with the cutting forces themselves. The ADAMS solver predicts the status of the machine, integrating the motion equations. The positions and the velocities of the points in contact with the soil are then outputted and transferred to Simulink, to compute the forces acting on the tracks and on the cutting picks. These forces are then again fed to the ADAMS model to complete another integration step. Detailed descriptions of the two sub-models are provided below.

3.1. Model of the machine

A multi-body model of the surface miner was developed in the ADAMS environment. The model describes the 3D motion of the machine, taking into account the flexibility of the chassis (by including it as super-elements in a non-linear multi-body analysis, as explained more fully below). This makes it possible to include the effect of the flexibility of the structure that supports the cutter head on the cutting forces.

While this practice is well-established in the field of metal machining [27,38], rock cutting modelling has not yet been extended in this direction. The models for computation of rock cutting forces, indeed, do not consider the possible contribution of the deformation of the structure supporting the cutter head. The most complete approach to fill this gap would be to model both the structure's flexibility and the machine's power generation/transmission; however, a first step was taken by introducing the machine structure's deformability into the model. However, the power generation and transmission chain were replaced with a simpler approach: the machine's travelling velocity and the drum's angular velocity were set as constant parameters in the analysis. This is clearly an important simplification, but it can be tolerated if the power estimated by means of the simulations is within the machine's capabilities.

The ADAMS/Flex capability of including flexible elements in the multi-body model was exploited, by importing the super-element matrices of the machine's main assemblies from the FE ANSYS model. The algorithm used is based on component mode synthesis, according to the Craig and Bampton's approach [39]. This method reduces the size of a finite element model, describing

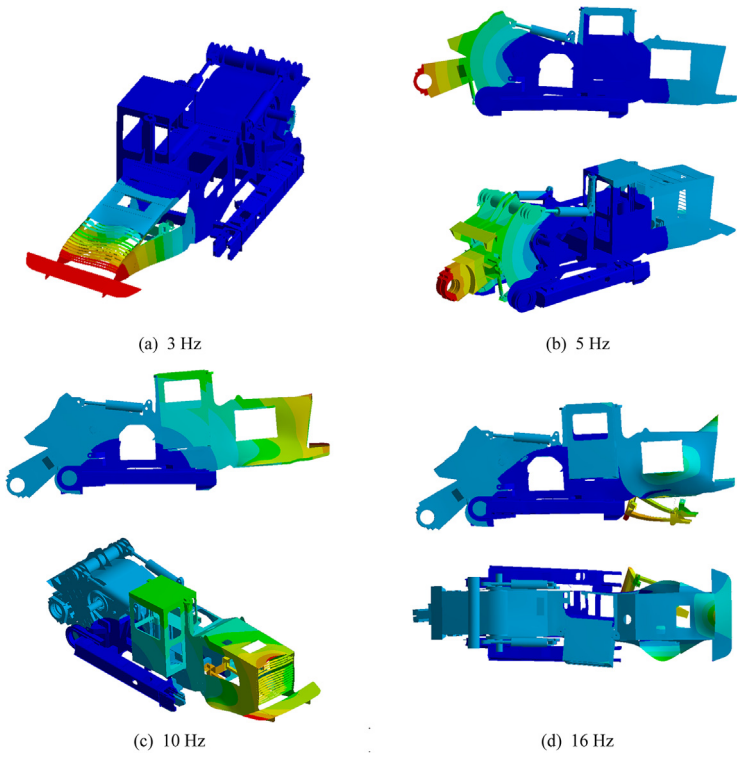

Fig. 4. Most relevant mode shapes of the Tesmec 1150XHD RH.

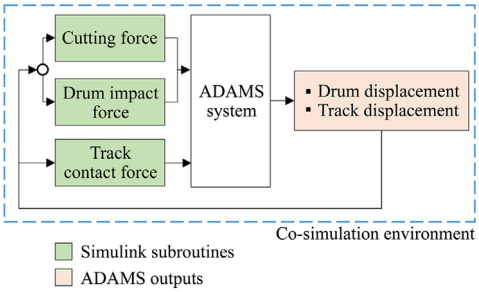

Fig. 5. Interaction between sub-models.

its motion with a combination of eigenmodes and static modes; the latter are obtained by applying unary displacements to the interface nodes, i.e., nodes that represent the boundary of the system where forces with other systems are transmitted. Both rigid and flexible bodies were included in the model: the frame, the undercarriage, the boom and the boom holder were imported as flexible bodies. The cabin was modelled as a rigid body.

Gravity acceleration was managed by ADAMS, while the cutter head-terrain interaction forces were defined as variables, to be managed by a Simulink algorithm. The following boundary conditions were applied:

(1) Tractor displacement in a longitudinal direction is characterised by a constant forward speed v_{tract}.
(2) The tracks' contact forces were applied to the rollers interface points, with a penalty algorithm (Eqs. (2) and (3), with reference to Fig. 6.

The normal and lateral forces exchanged between the tracks and the ground are computed as follows. The normal contact force (in the z direction) is given by:

$$\vec{F}_{\text{track}-z} = \sum_{i=1}^{n_{\text{roll}}} \left[k_{\text{ground}} \left(-\Delta \vec{u}_{\text{roll}-z,i} \right) + c_{\text{ground}} \left(-\vec{v}_{\text{roll}-z,i} \right) \right] \tag{2}$$

where $\vec{F}_{\text{track}-z}$ is the contact force in the z direction; n_{roll} the number of rollers in contact with the terrain; k_{ground} the contact stiffness; $\Delta \vec{u}_{\text{roll}-z,i}$ the penetration of the i^{th} roller; c_{ground} the contact damping coefficient; and $\vec{v}_{\text{roll}-z,i}$ the i^{th} roller velocity in the z direction.

The rock's contact stiffness was computed from the rock elasticity modulus and contact area. The track's lateral contact force, on the other hand, is obtained as:

$$\vec{F}_{\text{roll}-y,i} = \mu_{\text{ground}} \left(-\frac{\vec{v}_{\text{roll}-y,i}}{|\vec{v}_{\text{roll}-y,i}|} \right) \vec{F}_{\text{roll}-z,i} \tag{3}$$

where $\vec{F}_{\text{roll}-y,i}$ is the i^{th} roller contact force in the y direction; μ_{ground} the contact friction coefficient assumed equal to 0.6 [40]; $\vec{v}_{\text{roll}-y,i}$ the velocity of the i^{th} roller in the y direction; and $\vec{F}_{\text{roll}-z,i}$ the i^{th} roller contact force in the z direction.

3.2. Model of the cutting force

Rock cutting has been extensively studied, from the first works by Evans [11] through to recently. The research has focused on models to predict cutting forces [4,19,41,42], both in rock and coal excavation [43]. Process optimization has been given great relevance too [44,45], because of both the economic [43] and environmental implications of more efficient machines. However, very little relevance has been given to the vibrations induced by the material-structure interaction, while this aspect has been extensively investigated in metal machining [27,38]. The model implemented in this work aims to estimate how the chassis's vibrations influence the cutting forces and vice versa.

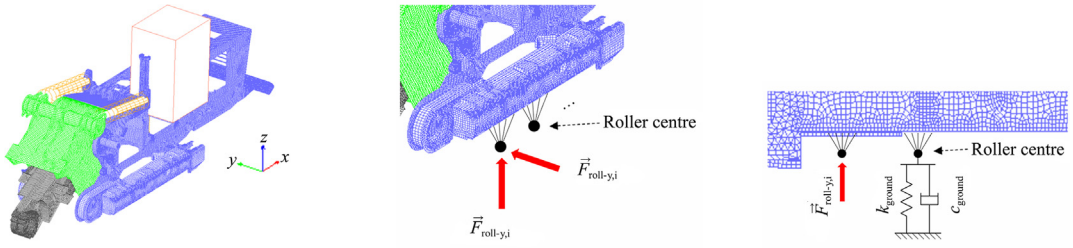

(a) ADAMS model: general view

(b) Contact forces and detail of the vertical force penalty algorithm implementation

Fig. 6. ADAMS model details.

3.2.1. Models for predicting rock cutting forces

The models proposed in literature can be divided into four main categories: analytical, semi-empirical, empirical and numerical. Most of these models were developed and validated using experimental data obtained from linear cutting tests (LCTs), which is the most common method reported in literature [4] for measuring cutting actions in a laboratory environment. LCT machines usually have a very stiff structure and the method consists of cutting straight trajectories on a sample of rock, using a cutting pick which is connected to a force measuring device. The models most relevant to this work, i.e., regarding conical picks, will be introduced below.

A theoretical model, based on the elastic fracture mechanics theory, was proposed by Bao et al. [13]. The chip shape was established based on the maximum tensile criterion and on a relationship between the vertical fracture angle and its associated parameters. One of the most complete empirical formulations, is the one proposed by Shao [15]. Here, a multiple linear regression correlates a large number of parameters, including the cutting speed (Eqs. (4) and (5)).

$$F_{c,m} = 1.716 - 0.081 \cdot \theta_a + 0.426 \cdot doc + 0.042 \cdot s + 0.681 \cdot v_c \quad (4)$$

$$F_{n,m} = 9.372 - 0.282 \cdot \theta_a + 0.490 \cdot doc + 0.077 \cdot s + 2.342 \cdot v_c \quad (5)$$

where $F_{c,m}$ is the mean cutting force; $F_{n,m}$ the mean normal force; θ_a the attack angle; doc the depth of cut; s the lateral spacing; and v_c the tangential velocity.

Several numerical approaches were also developed: while requiring a huge calibration effort, they can deliver very accurate results and insight into the process's mechanics. One of the most promising methods is DEM simulation [18–20].

3.2.2. Modelling of cutting dynamics

The problem of studying cutting dynamics has been paramount in the field of metal milling, because of its influence on the surface quality of the cut pieces [28]. What has been found is that the frequency input to the structure is dependent on the cutting parameters [29]. The cutting phenomenon is non-linear, and the frequency of the spindle's angular speed and its multiples are expected in the force signal. Moreover, new frequencies are added to the response spectrum, when the milling process is in a region of dynamic instability [27,30].

Modelling milling process dynamics requires taking the influence of the structure's response into account, especially at high feed rates. Several modelling techniques have been published in literature, from analytical [29] (with use of delayed differential equations (DDEs)) to numerical methods [38]. The idea in literature [29] is to include computation of the forces due to the cutting process, in the system equilibrium equations, as a function of the chip thickness. One of the most interesting examples of complete process simulation is that reported by Lee et al. [38] in which all three system dimensions (the machine's dynamic response, the cutting process and the control system) are reproduced in the model.

3.2.3. Implemented cutting force model

The implemented model starts computing the kinematic depth of cut of each pick, starting from the cutting parameters. This is done by reproducing the picks' kinematics during the excavation and by properly scaling the theoretical depth of cut, to consider the picks' interactions. The following steps are applied:

(1) Setting of the cutting parameters: tractor velocity, drum angular velocity, picks positions and angles, cutter head radial immersion and material characteristics.
(2) Computing the trajectory of each pick and the amount of material cut (theoretical depth of cut).
(3) Computing the effective amount of material cut by each pick (considering the possible interactions between tool and rock).

Some assumptions were made: the rock chip shape was taken according to Evans [11] (60° breakout angle) and the cutting parameters were not influenced by effects due to rock breaking mechanics. The theoretical depth of cut of each pick was computed by applying the method suggested by Sun et al. [16]. The collaboration of adjacent picks in material excavation, was computed using the breakout plane representation technique [16]. The effective removed area for each tool was then calculated (Fig. 7).

The effective depth of cut was computed as shown in Eq. (6), as reported by Hekimoglu [42].

$$doc_{\text{eff}}(t) = doc_{\text{theo}}(t)\frac{A_{\text{eff}}(t)}{A_{\text{theo}}(t)} \quad (6)$$

where $A_{\text{theo}}(t)$ is the theoretical removed area (not considering picks' interactions); and $A_{\text{eff}}(t)$ the effective removed area.

Given its large parameters set, Shao's model (Eqs. (4) and (5)) was selected to compute the cutting force in the simulation. Here doc (depth of cut) was replaced with the dynamic depth of cut $doc_{\text{dyn},i}$. The dynamic depth of cut is indeed influenced by the cutter head translation, due to the vibrations of its supporting structure. This concept is expressed by Eq. (7), with reference to Fig. 8.

$$doc_{\text{dyn},i}(t) = doc_{\text{eff},i} + \Delta doc_i(t) \quad (7)$$

Shao's model is derived from LCT data, and this means that the cutting forces computed in Eqs. (4) and (5) do not consider any dynamic effect due to the cutter head's vibrations. To include the effect of pick-material impacts, a penalty contact interaction was used (Eq. (8), with reference to Fig. 8).

$$\vec{F}_{\text{imp}} = \sum_{i=1}^{n_{\text{picks,cut}}} \left[k_{\text{ind}}\left(-\Delta\vec{u}_{p,i}\right) + c_{\text{ind}}\left(-\vec{v}_{p,i}\right)\right] \cdot \vec{n}_{\text{pick},i} \quad (8)$$

where $\vec{F}_{\text{imp}}$ is the resultant force acting on the drum due to the picks impacting with the ground; $n_{\text{picks,cut}}$ the number of picks cut-

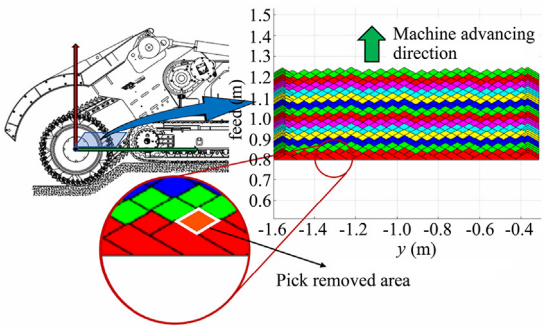

Fig. 7. Computation of the effective removed area, using the breakout plane technique.

ting; k_{ind} the indentation stiffness of the rock, the value of which was taken from literature, from indentation tests on sandstone samples (22000 N/mm) [13]; c_{ind} a very small value that was introduced mainly to stabilize the simulation. Reliable data on the material damping coefficient was not available; and $\Delta\vec{u}_{p,i}$ the penetration of the pick, varying during the numerical simulation as a function of the relative position between cutting head and rocky soil.

4. Results

The numerical model was used to analyze the interaction between the cutting forces and the dynamics of the chassis. The results obtained from the model were compared with experimental data collected during the excavation process in a rock quarry. The model was then used to perform a sensitivity analysis by changing the cutting parameters.

4.1. Experimental tests

Experimental data was obtained from an experimental campaign, carried out to measure the system's dynamics, as a function of the most relevant variables that influence its behaviour. A Tesmec 1150XHD RH machine was fitted with instruments and tested in a dolomite rock quarry, to capture both the input and the output of the system. A total of 89 signals were measured, aimed at characterizing both the machine's response and the cutting process. The most meaningful signals are listed in Table 1. The machine was equipped with accelerometers to characterize the vibrating response of the chassis. The hydraulic transmission was fitted with instruments to measure the drum rotating speed and the pressures of the hydraulic motor; these measurements made it possible to estimate the torque on the drum resulting from the cutting forces acting simultaneously on several cutting tools. In addition, dynamometric cutting tools were set-up by introducing load cells between the picks and the drum. These load cells were custom-designed to be tri-axial load cells, measuring the force applied to the digging pick in three directions. They were installed on the cutter head, replacing some of the standard picks' supporting blocks. The shape of the blocks was modified to create stress intensification points, where strain gauges were applied. The load cells were then calibrated with laboratory equipment. It was therefore possible to measure the cutting force on some tools.

In order to explore the machine's behaviour for a meaningful range of operating conditions, nearly 400 experiments were carried out under the conditions listed in Table 2.

The site chosen for the tests was a dolomite rock quarry, which is very representative of the machine's operating environment. The site was adequately prepared to remove any layers of altered rock, and it was levelled with the aid of a 3D GPS system. The acquisition parameters were set in order to guarantee:

(1) Maximum measurable frequency (excluding hydraulic pressure and machine control signals) = 2000 Hz.
(2) Maximum measurable frequency of pressures and machine control = 225 Hz.
(3) Frequency resolution = 0.017 Hz.

4.2. Pick force and cutter head resultant force

Fig. 9 shows the measured cutting force against the simulated one, in both the time and frequency domain. The experimental data was collected with the following parameters: d_{drum} = 350 mm, ω_{drum} = 36 r/min, v_{tract} = 5 mm/s, s = 28 mm. The two signals match well, in particular:

(1) The shape of simulated force signal in the time domain is consistent with the cycloidal trajectory of the cutting tool: it has its maximum at the beginning of the digging arch and returns to zero at the end of it.
(2) The cutting time, that is the time spent in contact with the material, is the same for both the experimental and the numerical force.
(3) A very good match is observed in the frequency domain for both the position and the spacing of the peaks; moreover, the effect of the cutter head's revolution frequency is well reproduced.
(4) The effect of the chassis's dynamics is evident and also well reproduced in the 4–8 Hz range, that is the frequency interval influenced by the machine's first pitch mode.
(5) The amplitude of the simulated peak force is higher for lower frequencies and the reason for this can be understood by looking at the time domain results (Fig. 9a). As shown in Fig. 9a, despite being the maximum values of the numerical force being lower than the experimental ones, the shape of the numerical force signal is more continuous. This is due

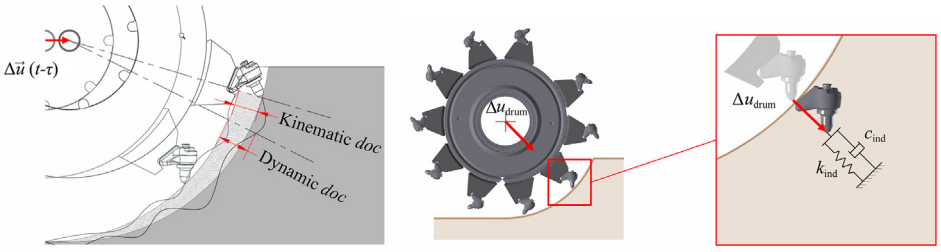

(a) Variation of the dynamic depth of cut with the cutter head's translation

(b) Penalty contact interaction applied to the pick's impact force

Fig. 8. Dynamic vs. kinematic depth of cut and pick-terrain interaction.

Table 1
Summary of the signals measured on the Tesmec 1150XHD RH instrument-equipped machine.

Target measurement	Measuring device
Cutter head transmission dynamics	Instrument-equipped digging gearbox - Fast shaft velocity and acceleration - Pressure probes on hydraulic motor in and out ports
Structure accelerations	Accelerometers in relevant locations
Pick cutting force	Load cells mounted between picks and cutter head's drum
Machine control parameters	Engine load factor Engine rotaition per minute Control settings

Table 2
Variables and values of the experiment domain.

Parameter	Value
d_{drum} (mm)	150, 250, 350
ω_{drum} (r/min)	18, 24, 30, 36
v_{tract} (mm/s)	5, 12, 20
s (mm)	28, 57
d_{pick} (mm)	16, 19

to the cutting force formulation that computes average forces, i.e., the chipping process is not reproduced in the model. The discontinuous nature of the cutting force signal is shown in Fig. 10 which reports the time history of the cutting force recorded by one of the load cells mounted between the pick and the drum.

Similar results were also found in the other testing conditions, with a general underestimation of the (absolute) peaks of the cutting force; the numerical model tends to predict smoother forces, the harmonic content of which is characterized by larger amplitudes for frequencies below 2–3 Hz, and vice versa for frequencies above 10 Hz. In any case, the duration of the contact between cutting tools and rock is consistent between the experimental and the numerical results. In addition, the effect of the vibrational response of the machine is clearly visible and consistent as well.

As an additional result, Fig. 11 shows the numerical-experimental comparison for a different set of cutting parameters: d_{drum} = 350 mm, ω_{drum} = 36 r/min, v_{tract} = 12 mm/s, s = 28 mm; the forward speed is thus increased by 7 mm/s compared to previous case. The remarks made about Fig. 9 also apply to Fig. 11, regarding the smoothness of simulated signals and the amplitude of harmonic components. In this case, the numerical-experimental

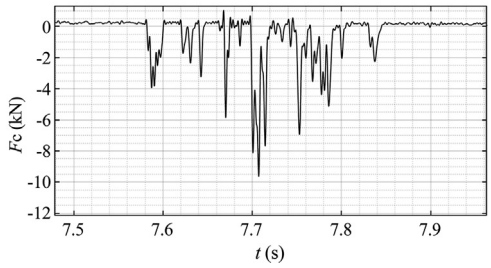

Fig. 10. Detail of experimental pick cutting force.

match is less good, but still the frequency spacing and the amplitudes of the most important frequency components are well approximated, given the uncertainty of the experimental condition in the field. Comparing the spectra reported in Fig. 9b and Fig. 11b, clearly highlights how the interaction between cutting forces and chassis's dynamics changes when different cutting parameters are set: while the effect of the machine's first pitch mode is evident in Fig. 9b, its role appears less important in Fig. 11b. It is noteworthy that the numerical model is consistent with experimental data as far as this outcome is concerned.

4.3. Depth of cut and resulting cutting forces

Even though the effect of the chipping process was not modelled, thus incurring in the issue of reproducing a force that is smoother that the experimental one, the proposed model is a great improvement on the purely kinematic approach. Fig. 12 shows the comparison between the pick depth of cut, computed by the kinematic and the multi-body models. Recalling that the depth of cut is one of the main parameters the excavation forces depend on, the following can be observed:

(1) The kinematic depth of cut is by no means influenced by the cutter head's dynamics, thus presenting a shape which only depends on the cycloidal trajectory of the pick.
(2) The dynamic depth of cut, computed using the multi-body model, is able to reproduce the *doc* variation due to the movement of the drum, when the pick is cutting.
(3) The dynamic depth of cut computed by the multibody model is able to reproduce the loss of contact between the pick and the rock, zeroing the excavation forces (negative depth of cut).

When the influence of the machine's dynamics on the depth of cut of the picks is taken into consideration, it has an impact on the

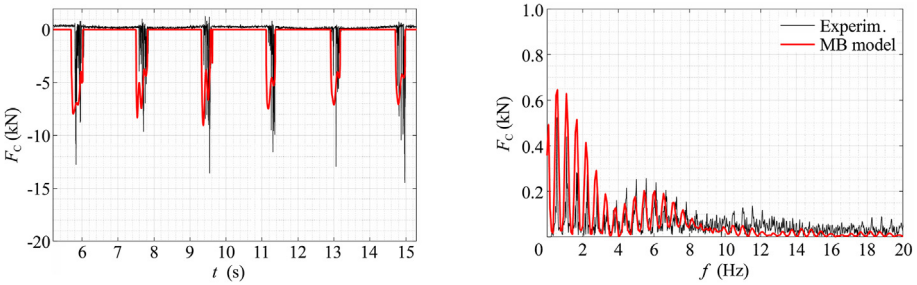

(a) Numerical vs. experimental: pick cutting force, in the time domain

(b) Numerical vs. experimental: pick cutting force, in the frequency domain

Fig. 9. Numerical vs. experimental: pick cutting force.

As noted in Fig. 9, the cutting parameters are as follows: d_{drum} = 350 mm, ω_{drum} = 36 r/min, v_{tract} = 5 mm/s, and s = 28 mm.

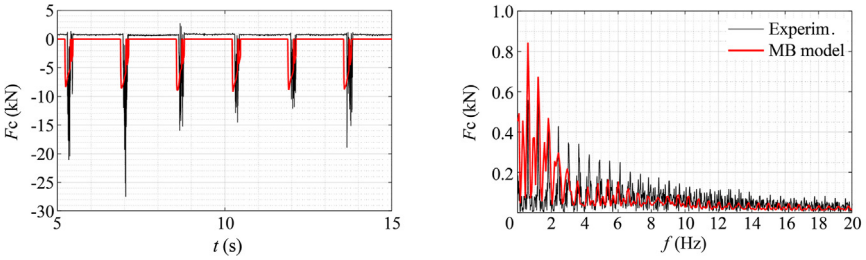

(a) Numerical vs. experimental: pick cutting force, in the time domain

(b) Numerical vs. experimental: pick cutting force, in the frequency domain

Fig. 11. Numerical vs. experimental: pick cutting force.

As shown in Fig. 11, the cutting parameters are as follows: d_{drum} = 350 mm, ω_{drum} = 36 r/min, v_{tract} = 12 mm/s, and s = 28 mm.

resultant force calculation. The resultant force at the cutter head's support is computed as the vector sum of all the forces acting on the cutting tools. The kinematic resultant computation does not consider the influence of the depth of cut variation, and this makes the kinematic resultant force much larger and much more stable than that computed using the multi-body model (Fig. 13). The result in Fig. 13 highlights how variations in the resultant force are deeply influenced by the interaction between the cutting forces and the dynamic response of the surface miner. This is an important achievement as it shows that the amplitude and the number of load cycles are significantly reduced when that interaction is neglected. Therefore, taking this phenomenon into account at the design stage, clearly modifies the prediction of the component's fatigue life.

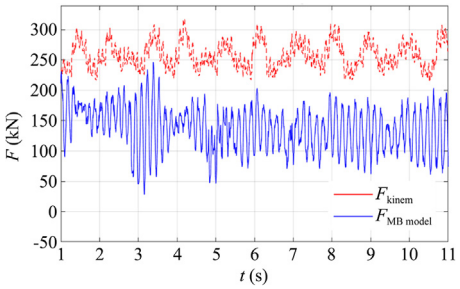

Fig. 13. Simulated cutter head resultant force, kinematic model vs. multi-body model.

As illustrated in Fig. 13, the cutting parameters are as follows: d_{drum} = 350 mm, ω_{drum} = 36 r/min, v_{tract} = 5 mm/s, and s = 28 mm.

4.4. Cutting torque

Fig. 14 shows the comparison between the numerical and the experimental cutter head torques, in both the time and frequency domain. The following can be observed:

(1) A good match is found for the peaks' locations in the frequency domain.
(2) The signals' oscillation amplitudes, in the time domain, are of the same order of magnitude, while the average value of the numerical torque is larger.
(3) The amplitude of the peaks is larger for the numerical results, but still in the same order of magnitude as the experimental ones.

The explanation of the differences between the numerical and the experimental torque can be found in the assumptions of the multi-body model: the chipping process features are not reproduced in the cutting force computation; all the picks are cutting in the exact same conditions and on the same idealized material. No variability in the material strength or characteristics is considered as a function of the picks' location. These two elements ultimately lead to the computation of a cutting torque that is higher than the real one.

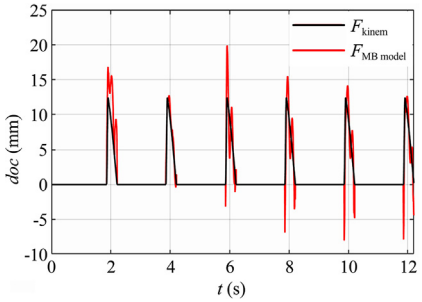

Fig. 12. Kinematic vs. dynamic (multi-body model) simulation: depth of cut.

As noted in Fig. 12, the cutting parameters are as follows: d_{drum} = 350 mm, ω_{drum} = 36 r/min, v_{tract} = 5 mm/s, and s = 28 mm.

4.5. Chassis's dynamic response

In order to validate the model, the acceleration at point A (Fig. 15) was also investigated. Moreover, the coherence between the acceleration's amplitude and the variation of the track's velocity was checked too. For the chassis's accelerations, a comparison between the numerical results and the experimental data was carried out at point A on the machine's frame, close to the diesel engine (Fig. 15).

The comparison is provided in Fig. 16, which shows that the numerical and the experimental signals exhibit a good match, in terms of both the amplitude and the locations of the peaks. This is true for the x and z directions, while the signals in the y direction are less consistent, probably because no lateral cutting force was implemented in the model. It is very interesting to observe how the vibrating content predicted by the model, in both the longitudinal and vertical direction, is consistent with that measured during the tests. The vibrating mode at 5 Hz, which involves a significant displacement of the boom (Fig. 4), introduces an important contribution to the vibration of the chassis. This proves that the model can also correctly predict the vibration amplitudes produced in locations far from the cutting head, which is very important, as this allows a consistent evaluation of the fatigue stresses on the chassis.

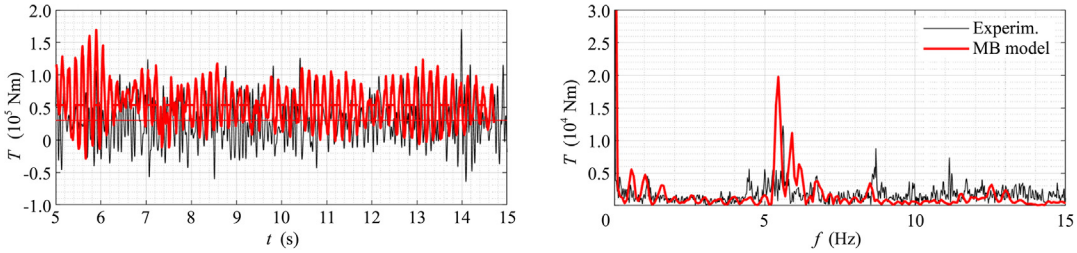

(a) Numerical vs. experimental: cutting torque, in the time domain

(b) Numerical vs. experimental: cutting torque, in the frequency domain

Fig. 14. Numerical vs. experimental: cutting torque.

As illustrated in Fig. 14, the cutting parameters are as follows: d_{drum} = 350 mm, ω_{drum} = 36 r/min, v_{tract} = 5 mm/s, and s = 28 mm.

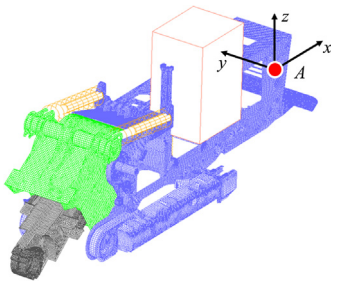

Fig. 15. Location of the reference measured accelerations.

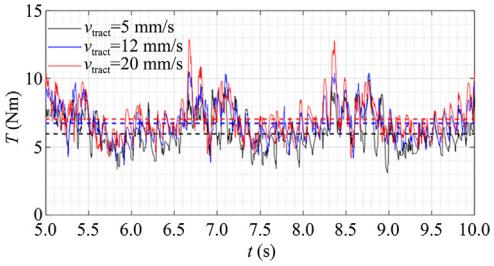

Fig. 17. Simulated cutting torque, for three different values of tractor translating velocity (d_{drum} = 0.35 m, ω_{drum} = 36 r/min, s = 28 mm) and the dashed lines shown as the average torque value.

4.6. Response to a variation in parameters

In order to understand the model's capability of reproducing the machine's behaviour for different cutting parameters, a preliminary sensitivity analysis was carried out. Fig. 17 shows the cutter head torque computed with three different velocities of tractor translation. The other parameters of the simulations were set as: d_{drum} = 0.35 m, ω_{drum} = 36 r/min, s = 28 mm. According to what was found by the authors in the experimental tests, the average cutting torque increases when the feed does. In this case indeed, increasing the tractor's velocity, while keeping the drum's angular velocity constant, corresponds to increasing the cutting feed. The dashed lines in Fig. 17 correspond to the average torque values which increase with track velocity.

The simulations were carried out with two different values of drum depth, and three different values of tractor translation velocity. The other parameters of the simulations were set as: ω_{drum} = 36 r/min, s = 28 mm. Fig. 18 shows the result of varying the track velocity: varying the track velocity not only increases the forces input to the structure and thus the vibration amplitude, but also increases the average compression force acting on the boom's hydraulic actuator. As a consequence, the first pitch frequency is shifted, because a greater compression on the actuator means a stiffer structure. Both these behaviours can be seen in Fig. 18.

Fig. 19 shows the results of varying both the track velocity and the drum depth. The zoomed view presented in Fig. 19b clearly reveals how the drum depth of cut causes an increase in the vibration amplitude.

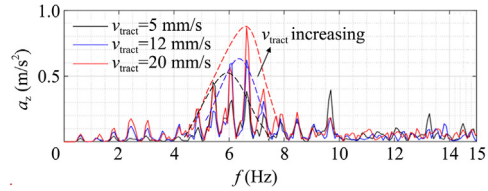

Fig. 18. Simulated frame acceleration a at point A, for three different values of tractor translating velocity (d_{drum} = 0.35 m, ω_{drum} = 36 r/min, s = 28 mm).

5. Conclusions

In this work, an effort was made to improve the capability of modelling rock cutting equipment. In particular, the focus was on characterizing the influence of the structure's flexibility on the process dynamics. This goal was pursued by studying a 1150XHD RH rock milling machine, or surface miner, produced by the Tesmec company. In particular:

(1) A machine dynamic model was developed with the goal of computational efficiency, in order to make it a tool suitable for use in the design phase. For this reason, only empirical cutting force models were chosen.
(2) An algorithm was implemented to compute the tool trajectory and the effective depth of cut. The effect of the structure's deformability and of the non-linearities, due to the machine boundary conditions, were included, by imple-

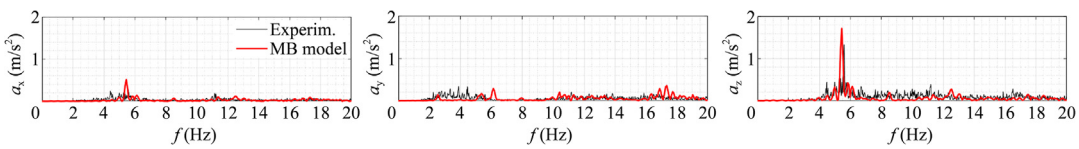

Fig. 16. Numerical vs. experimental accelerations a on the machine's frame at point A.

As illustrated in Fig. 16, the cutting parameters are as follows: d_{drum} = 350 mm, ω_{drum} = 36 r/min, v_{tract} = 5 mm/s, and s = 28 mm.

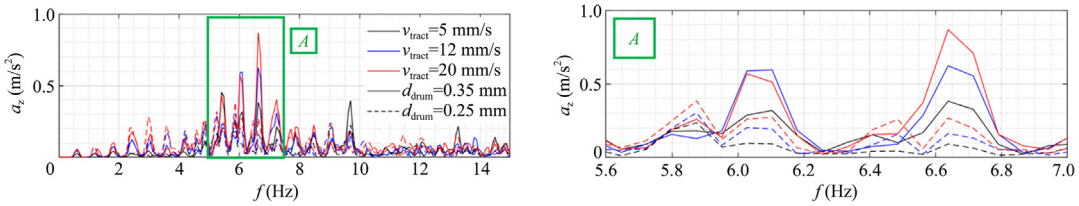

Fig. 19. Simulated frame acceleration a at point A, for three different values of tractor translating velocity and two values of drum depth (ω_{drum} = 36 r/min, s = 28 mm).

menting a flexible multi-body model. Here, the kinematic trajectories of the picks were corrected with the effect of the machine's dynamics and the excavation forces were computed by applying models from literature.

(3) From the comparison of the numerical results and the experimental data, the following was observed.
Including the effect of the chassis dynamics led to an improvement on the kinematic approach in literature: fluctuations in the force values were indeed observed, due to both the chip thickness variation as well as the pick-rock contact separation.
The cutting forces predicted using the numerical model display a good match with the experimental data, especially in the frequency range influenced by the machine's dynamics. The amplitude of the simulated cutting forces is generally slightly larger than the experimental one. This difference is due to the fact that the chipping process (the mechanics of the chip creation) is not reproduced by the model and this makes the simulated signals smoother, with larger average values.
The model is sensitive to the variation of the process parameters, reproducing the trends identified in the experimental data analysis.

Altogether, a useful design tool was developed, leading to a deeper insight into the interaction between machine dynamics and cutting process. Some improvements could be introduced anyway, to increase the model's accuracy. Firstly, a proper model of the powertrain should be included: this would lead to a better prediction of the load fluctuations on one hand, while improving the modelling of the tractor boundary conditions on the other. Secondly, the cutting force calculation model could be improved as well, by using a fracture mechanics approach and imposing the chip shape on a statistical basis, for example introducing chip size statistics, or by using a numerical approach, like DEM.

References

[1] Buffington GL. The Art of Blasting on Construction and Surface Mining Sites. The Art of Blasting on Construction and Surface Mining Sites. Orlando, Florida: American Society of Safety Engineers; 2000.
[2] Yao Q. An investigation of rock cutting: towards a novel design of cutting bits. Sydney: The Unversity of New South Whales; 2012. Doctorial dissertation.
[3] Inyang H. Developments in Drag Bit Cutting of Rocks for Energy Infrastructure. Int J Surf Min Reclam Environ 2002;16:248–60.
[4] Bilgin N, Demircin M, Copur H, Balci C, Tuncdemir H, Akcin N. Dominant rock properties affecting the performance of conical picks and the comparison of some experimental and theoretical results. Int J Rock Mech Min Sci 2006;43:139–56.
[5] Leng Z, Fan Y, Gao Q, Hu Y. Evaluation and optimization of blasting approaches to reducing oversize boulders and toes in open-pit mine. Int J Min Sci Technol 2020;30:373–80.
[6] Quentin Eades R, Perry K. Understanding the connection between blasting and highwall stability. Int J Min Sci Technol 2019;29:99–103.
[7] Bilgin N. Mechanical Excavation in Mining and Civil Industries. CRC Press; 2014.
[8] Prakash A, Murthy VMSR, Singh KB. A new rock cuttability index for predicting key performance indicators of surface miners. Int J Rock Mech Min Sci 2015;77:339–47.
[9] Danial JA, Mohammadreza K, Aminaton M, Saffet Y. Application of several optimization techniques for estimating TBM advance rate in granitic rocks. J Rock Mech Geotech Eng 2019;11(4):779–89.
[10] Kumar C, Kumaraswamidhas LA, Murthy VMSR, Prakash A. Experimental investigations on thermal behavior during pick-rock interaction and optimization of operating parameters of surface miner. Int J Rock Mech Min Sci 2020;133:104360.
[11] Evans I. A theory of the cutting force for point-attack picks. Int J Min Eng 1984;2:63–71.
[12] Liu S, Du C, Cui X. Research on the cutting force of a pick. Min Sci Technol 2009;19. 524 517.
[13] Bao R, Zhang L, Yao Q, Lunn J. Estimating the Peak Indentation Force of the Edge Chipping of Rocks Using Single Point-Attack Pick. Rock Mech Rock Eng 2011;44(3):339–47.
[14] Yasar S, Yilmaz AO. Drag pick cutting tests: A comparison between experimental and theoretical results. J Rock Mech Geotech Eng 2018;10:893–906.
[15] Shao W. A study of rock cutting with point attack picks. Brisbane: University of Queensland; 2016. Doctorial dissertation.
[16] Sun Y, Li X, Shao W. Influence of cutting parameters and interactions on the depth of cut in continuous mining operation. Adv Mater Res 2012;538–541:1422–8.
[17] Menezes PL, Lovell MR, Avdeev IV, Higgs CF. Studies on the formation of discontinuous rock fragments during cutting operation. Int J Rock Mech Min Sci 2014;71:131–42.
[18] Li X, Zhao J. An overview of particle-based numerical manifold method and its application to dynamic rock fracturing. J Rock Mech Geotech Eng 2019;11(3):684–700.
[19] Rojek J, Onate E, Labra C, Kargl H. Discrete element simulation of rock cutting. Int J Rock Mech Min Sci 2011;48(6):996–1010.
[20] Huang H, Detournay E. Discrete element modeling of tool-rock interaction II: rock indentation. Int J Numer Anal Meth Geomech 2013;37(13):1930–47.
[21] Mohammadnejad M, Dehkhoda S, Fukuda D, Liu H, Chan A. GPGPU-parallelised hybrid finite-discrete element modelling of rock chipping and fragmentation process in mechanical cutting. J Rock Mech Geotech Eng 2020;12(2):310–25.
[22] Abousleiman R, Walton G, Sinha S. Understanding roof deformation mechanics and parametric sensitivities of coal mine entries using the discrete element method. Int J Min Sci Technol 2020;30:123–9.
[23] Fowell N, Ochei R. A comparison of dust make and energy requirements for rock cutting tools. Geotech Geol Eng 1984;2:73–83.
[24] Deshmukh S, Raina AK, Murthy VMSR, Trivedi R, Vajre R. Roadheader– A comprehensive review. Tunn Undergr Space Technol 2020;95:103148.
[25] Ling J, Sun W, Huo J, Guo L. Study of TBM cutterhead fatigue crack propagation life based on multi-degree of freedom coupling system dynamics. Comput Ind Eng 2015;83:1–14.
[26] Jovančić PD, Ignjatović D, Tanasijević M, Maneski T. Load-bearing steel structure diagnostics on bucket wheel excavator, for the purpose of failure prevention. Eng Fail Anal 2011;18:1203–11.
[27] Stépán G, Dombovari Z, Munoa J. Identification of cutting force characteristics based on chatter experiments. Cirp Annals-manufacturing Technology 2011;60(1):113–6.
[28] Çomak A, Budak E. Modeling dynamics and stability of variable pitch and helix milling tools for development of a design method to maximize chatter stability. Precision Eng-J Int Soc Precision Eng Nanotechnol 2017;47:459–68.
[29] Insperger T, Mann BP, Stepan G, Bayly P. Stability of up-milling and down-milling, part 1: alternative analytical methods. Int J Mach Tools Manuf 2003;43:25–34.
[30] Eynian M. Vibration frequencies in stable and unstable milling. Int J Mach Tools Manuf 2015;90:44–9.
[31] Barnewold L, Lottermoser BG. Identification of digital technologies and digitalisation trends in the mining industry. Int J Min Sci Technol 2020;30(6):747–57.
[32] Frimpong S, Thiruvengadam M. Multibody Dynamic Stress Simulation of Rigid-Flexible Shovel Crawler Shoes. Minerals 2016;6(3):61.
[33] Dai Y, Pang L, Chen L, Zhu X, Zhang T. A New Multi-Body Dynamic Model of a Deep Ocean Mining Vehicle-Pipeline-Ship System and Simulation of Its Integrated Motion. Strojniški vestnik - J Mech Eng 2016;62(12):757–63.
[34] Melzi S, Negrini S, Sabbioni E. Numerical analysis of the effect of tire characteristics, soil response and suspensions tuning on the comfort of an agricultural vehicle. J Terramech 2014;55:17–27.

[35] Bennett N, Walawalkar A, Heck M, Schindler C. Integration of digging forces in a multi-body-system model of an excavator. Proc Inst Mech Eng Part K J Multi-body Dynamics 2016;230(2):159–77.
[36] Dopico D, González ALP. A soil model for a hydraulic simulator excavator based on real-time Multibody dynamics. In: Proceedings of 5th Asian Conference on Multibody Dynamics. Kyoto, Japan; 2010.
[37] Xia YM, Guo B, Cong GQ, Zhang XH, Zeng GY. Numerical simulation of rock fragmentation induced by a single TBM disc cutter close to a side free surface. Int J Rock Mech Min Sci 2017;91:40–8.
[38] Lee C, Yang N, Oh C, Gim T, Ha J. An integrated prediction model including the cutting process for virtual product development of machine tools. Int J Mach Tools Manuf 2015;90:29–43.
[39] Craig R, Bampton M. Coupling of substructures for dynamic analysis. AIAA J 1968;6(7):1313–9.
[40] Rabbat B, Russel H. Friction coefficient of steel on concrete of grout. J Struct Eng 1985;3:505–15.
[41] Goktan R, Gunes N. A semi-empirical approach to cutting force prediction for point-attack picks. J S Afr Inst Min Metall 2005;105:257–64.
[42] Hekimoglu OZ. A pick force calculation method suggested for tool lacing of mechanical excavators employing drag tools. Int J Min Reclam Environ 2018;32(8):564–85.
[43] Liu S, Du C, Cui X, Song J. Experiment research on a new shearer drum. Procedia Earth Planet Sci 2009;1:1393–7.
[44] Rostami J, Ozdemir L. Roadheaders performance optimization for mining and civil construction. In: Proceedings of 13th Annual Technical Conference ISDT. Las Vegas; 1994.
[45] Du C, Liu S, Cui X, Li T. Study on pick arrangement of shearer drum based on load fluctuation. J China Univ Min Technol 2008;18:305–10.